Nearest-neighbor-spacing distribution of prime numbers and quantum chaos

Marek Wolf*

Cardinal Stefan Wyszynski University, Faculty of Mathematics and Natural Sciences. College of Sciences, ul. Wóycickiego 1/3, PL-01-938 Warsaw, Poland

(Received 15 January 2013; published 24 February 2014)

We give heuristic arguments and computer results to support the hypothesis that, after appropriate rescaling, the statistics of spacings between adjacent prime numbers follows the Poisson distribution. The scaling transformation removes the oscillations in the nearest-neighbor-spacing distribution of primes. These oscillations have the very profound period of length six. We also calculate the spectral rigidity Δ_3 for prime numbers by two methods. After suitable averaging one of these methods gives the Poisson dependence $\Delta_3(L) = L/15$.

DOI: 10.1103/PhysRevE.89.022922 PACS number(s): 05.45.Mt, 02.10.De

I. INTRODUCTION

The prime numbers often provided a toy model for some physical ideas of the past. For example, in Ref. [1] the multifractal formalism was applied to prime numbers, in Ref. [2] the appropriately defined Lyapunov exponents for the distribution of primes were calculated numerically. In Ref. [3] it was shown that the distribution of prime numbers displays $1/f$ noise, while in Ref. [4] $1/f^2$ noise was found in the difference between the prime-number-counting $\pi(x)$ function and Riemann's function $R(x)$. In Refs. [5] and [6] random walks on prime numbers were defined. In Ref. [7] an attempt to construct the dynamical model for prime numbers was taken and computable information content as well as entropy information of the set of prime numbers were calculated.

The prime numbers can be regarded as eigenvalues of some quantum Hamiltonian. The problem of construction of a simple one-dimensional Hamiltonian whose spectrum coincides with the set of primes was considered in Refs. [8–10]; see also the review in Ref. [11]. It is then natural to investigate the spacings between prime numbers, i.e., in physical language, the nearest-neighbor-spacing distribution (NNSD). Several authors have undertaken a study of this problem in the past; see Refs. [12–14]. Below we will treat prime numbers as the energy levels and we will apply methods used to describe statistical properties of discrete spectra. Let the quantum system possess the discrete spectrum $E_1, E_2, \ldots$ and let $N(E) = \sum_n \Theta(E - E_n)$ (Θ is a unit step function) denote the function counting the number of energy levels smaller than E. Usually spectral staircase $N(E)$ can be split into the "smooth" $\overline{N}(E)$ and fluctuating (oscillating) $\widetilde{N}(E)$ parts. For example, for a large class of differential operators on a d-dimensional bounded manifold $\Omega \subset \mathbb{R}^d$, Weyl's law,

$$\overline{N}(E) \sim \frac{\mathrm{vol}(\Omega)}{(2\pi)^d} E^{d/2}, \tag{1}$$

holds; see, e.g., Ref. [15] (chap. 1).

Given the spectrum $E_1, E_2, \ldots$, the statistics of normalized and dimensionless ("unfolded" spectrum; see, e.g., Ref. [16] (Sec. 4.7)) gaps between two consecutive energy levels $s_n = (E_{n+1} - E_n)/\overline{d}(E)$, where $\overline{d}(E)$ is the mean distance between energy levels up to E, has been extensively studied. For general systems, $E_{n+1} - E_n$ are arbitrary real numbers and a histogram of the level spacings s_n can be built. It is well known that level-spacing distributions of quantum systems can be grouped into a few universality classes connected with the symmetry properties of the Hamiltonians: Poisson distribution (i.e. e^{-s}) for systems with underlying regular classical dynamics, Gaussian orthogonal ensemble (GOE, also called the Wigner–Dyson distribution)—Hamiltonians invariant under time reversal, Gaussian unitary ensemble (GUE)—not invariant under time reversal and Gaussian symplectic ensemble (GSE) for half-spin systems with time reversal symmetry. There are many reviews on these topics, and we cite here Refs. [16–18].

There is some confusion regarding the proper statistics of the gaps between consecutive primes: In Ref. [12] it was claimed that the NNSD of primes follows a GOE distribution, while in Refs. [13,14] the possibilities of GOE, Poisson, and exotic Berry-Robnik [19] distribution were investigated. Liboff and Wong have obtained Wigner distribution and level repulsion for the NNSD of primes by artificially including the gaps 0 (no degeneracy—all primes differ) and 1; see Ref. [12] (p. 3113). Gap 1 appears only once between 2 and 3 and should be skipped in the wake of infinity of primes. There is a very often reproduced figure showing some typical spectra (see Refs. [17] (Fig. 12), [18] (Fig. 3), [20] (Fig. I.8), [21] (front figure), and [22] (p. 32)): random levels with no correlations (Poisson series), a sequence of prime numbers, resonance levels of the erbium-166 nucleus, the energies of a free particle in the Sinai billiard, and nontrivial zeros of the Riemann ζ function, respectively. In Ref. [17] (p. 10) it is stated that the "case of prime numbers ... are far from either regularly spaced uniform series or the completely random Poisson series with no correlations."

It is the purpose of this paper to settle "once and for ever" that the NSDD of primes follows the Poisson distribution. Section II is devoted to this problem. In Ref. [23] M. V. Berry has calculated spectral rigidity Δ_3 for zeros of the Riemann ζ function and in Sec. III we will study spectral rigidity for prime numbers.

II. NNSD FOR PRIME NUMBERS

In the case of prime numbers all gaps $d_n = p_{n+1} - p_n$ (except the first pair of primes $p_1 = 2, p_2 = 3$) are even integers $2,4,6,\ldots$. These spacings are dimensionless and we

*m.wolf@uksw.edu.pl

will not perform unfolding for the time being (see the next section)—the usual (17) unfolding obscures analysis of the oscillations present in the NNSD between original primes. Let $\tau_d(x)$ denote a number of pairs of *consecutive* primes smaller than a given bound x and separated by d,

$$\tau_d(x) = \sharp\{p_n, p_{n+1} < x, \quad \text{with} \quad p_{n+1} - p_n = d\}. \tag{2}$$

For odd $d = 2k+1$ we supplement this definition by putting $\tau_{2k+1}(x) = 0$.

In 1922, G. H. Hardy and J. E. Littlewood, in their famous paper [24], proposed 15 conjectures. Conjecture B of their paper states that there are infinitely many primes pairs (p, p'), where $p' = p + d$, for every even d. If $\pi_d(x)$ denotes the number of prime pairs differing by d and less than x, then

$$\pi_d(x) \sim C_2 \prod_{p|d} \frac{p-1}{p-2} \frac{x}{\ln^2(x)}. \tag{3}$$

Here $C_2 \equiv 2\prod_{p>2}(1 - \frac{1}{(p-1)^2}) = 1.32032\ldots$ is called the "twins constant."

In the middle of 2013, a major step towards the proof of conjecture B was made: Yitang Zhang submitted a paper to *Annals of Mathematics* in which he proved unconditionally that $\liminf_{n\to\infty}(p_{n+1} - p_n) < 7 \times 10^7$; see, e.g., Ref. [25]. Very soon this bound was lowered many times by mathematicians and the present record is $\liminf_{n\to\infty}(p_{n+1} - p_n) \leqslant 600$ and was obtained by J. Maynard [26].

Conjecture B of G. H. Hardy and J. E. Littlewood gives the number of pairs of primes that are not necessarily successive and we would like to stress that in (2) $\tau_d(x)$ denotes the number of pairs of *consecutive* primes p_n, p_{n+1} with difference $p_{n+1} - p_n = d$. The pairs of primes separated by $d = 2$ and $d = 4$ are special as they always have to be consecutive primes [with the exception of the pair (3,7), which contains 5 in the middle]: In the triple of integers $2k+1, 2k+3, 2k+5$ the middle $2k+3$ has to be divisible by 3 if $2k+1, 2k+5$ are prime (in particular, not divisible by 3). For $d = 6$ (and larger d) we have $\pi_6(x) > \tau_6(x)$, for example, (5,7,11),(7,11,13),(11,13,17),.... From the conjecture B of G. H. Hardy and J. E. Littlewood [24] it follows that the number of gaps $d = 2$ ("twins") is approximately equal to the number of gaps $d = 4$ ("cousins"), $\pi_2(x) \equiv \tau_2(x) \approx \pi_4(x) \equiv \tau_4(x)$; see also Ref. [6]. For $d \geqslant 6$ in Ref. [27] we have conjectured that

$$\tau_d(x) \sim C_2 \frac{\pi^2(x)}{x} \prod_{p|d, p>2} \frac{p-1}{p-2} e^{-d\pi(x)/x}$$
$$\text{for} \quad d \geqslant 6, \quad \tau_2(x)(\approx\tau_4(x)) \sim C_2 \frac{\pi^2(x)}{x} \approx C_2 \frac{x}{\ln^2(x)}. \tag{4}$$

Here $\pi(x) = \sum_n \Theta(x - p_n)$ denotes the number of primes up to x and, by use of the prime number theorem (PNT), is very well approximated by the logarithmic integral

$$\pi(x) \sim \mathrm{Li}(x) \equiv \int_2^x \frac{du}{\ln(u)}.$$

Integration by parts gives the asymptotic expansion which should be cut at the term $n_0 = \lfloor \ln(x) \rfloor$,

$$\mathrm{Li}(x) = \frac{x}{\ln(x)} + \frac{x}{\ln^2(x)} + \frac{2!x}{\ln^3(x)} + \frac{3!x}{\ln^4(x)} + \cdots. \tag{5}$$

There is a series giving $\mathrm{Li}(x)$ for all $x > 2$ and quickly convergent which has $n!$ in the denominator and $\ln^n(x)$ in the numerator instead of the opposite order in (5) [see Ref. [28] (Sec. 5.1)],

$$\mathrm{Li}(x) = \gamma + \ln\ln(x) + \sum_{n=1}^{\infty} \frac{\ln^n(x)}{n \times n!} \quad \text{for} \quad x > 1. \tag{6}$$

Here $\gamma = 0.577216\ldots$ is the Euler-Mascheroni constant.

Putting $\pi(x) \sim x/\ln(x)$ into (4), the compact formula expressing $\tau_d(x)$ by explicitly known functions

$$\tau_d(x) \sim C_2 \frac{x}{\ln^2(x)} \prod_{p|d, p>2} \frac{p-1}{p-2} e^{-d/\ln(x)} \tag{7}$$

is obtained. Comparing it with the original Hardy-Littlewood conjecture (3), we obtain that the number $\tau_d(x)$ of *successive* primes (p_{n+1}, p_n) smaller than x and of the difference $d(=p_{n+1} - p_n)$ is diminished by the factor $\exp(-d/\ln(x))$, in comparison with the number of *all* pairs of primes (p, p') apart in the distance $d = p' - p$,

$$\tau_d(x) \sim \pi_d(x) e^{-d/\ln(x)} \quad \text{for} \quad d \geqslant 6. \tag{8}$$

The expression (7) for $\tau_d(x)$ was proved (in slightly different form required by the precision of the formulation of the theorem) under the assumption of the conjecture B of Hardy-Littlewood by D. A. Goldston and A. H. Ledoan [29] in 2012.

During over a 7-month-long run of the computer program we have collected the values of $\tau_d(x)$ up to $x = 2^{48} \approx 2.8147 \times 10^{14}$. The data representing the function $\tau_d(x)$ were stored at values of x forming the geometrical progression with the ratio 2 at $x = 2^{15}, 2^{16}, \ldots, 2^{47}, 2^{48}$. Such a choice of the intermediate thresholds as powers of 2 was determined by the employed computer program in which the primes were coded as bits. The data are available for downloading from http://pracownicy.uksw.edu.pl/mwolf/gapstau.zip. The resulting curves are plotted in Fig. 1. Characteristic oscillating pattern of points is caused by the product

$$P(d) \equiv \prod_{p|d, p>2} \frac{p-1}{p-2}, \tag{9}$$

which appears in (4); see the inset in Fig. 1. This product appeared first in the paper of Hardy and Littlewood [24] and it has local maxima for d equal to the products of consecutive primes ("primorials," i.e., factorials over primes $2 \times 3 \times 5 \ldots \times p_n \equiv p_n\sharp$). Clearly visible in Fig. 1 are oscillations of the period $6 = 2 \times 3$ with overimposed higher harmonics $30 = 2 \times 3 \times 5$ and $210 = 2 \times 3 \times 5 \times 7$, i.e., when $P(d)$ has local maxima $P(6) = 2, P(30) = 8/3 = 2.666\ldots P(210) = 16/5 = 3.2$ (local minima are 1 and they correspond to $d = 2^m$). We have performed the discrete Fourier transform of $P(d)$, i.e., we calculated numerically

$$\widetilde{P}\left(\frac{n}{2M}\right) = \sum_{k=0}^{M-1} P(2k) e^{2\pi k n/M}, \tag{10}$$

where $n = 0, 1, 2, \ldots, M-1$ and $n/2M$ plays the role of discrete frequency. Having $\widetilde{P}(f)$, we can calculate the power spectrum density $S(f) = |\widetilde{P}(\frac{n}{2M})|^2$. The large value of $S(f)$ at some frequency f means that the dependence of $P(d)$

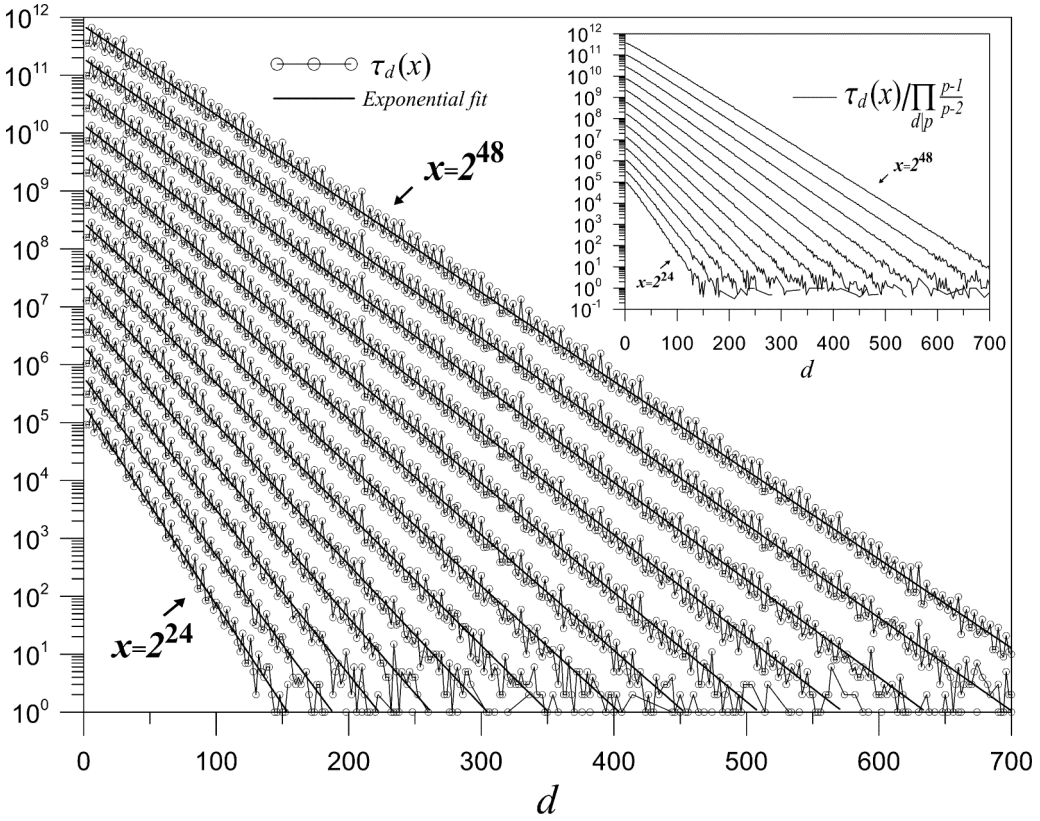

FIG. 1. Plots of $\tau_d(x)$ for $x = 2^{24}, 2^{26}, \ldots, 2^{46}, 2^{48}$. Wider lines represent exponential fits $a(x)e^{-db(x)}$ to $\tau_d(x)$. In the inset the plots of $\tau_d(x)/P(d)$ are shown.

on d has some harmonic component of the period $T = 1/f$. Thus in Fig. 2 we have plotted $S(f)$ versus $1/f = d$ to show the main periods $5{,}6 = 2 \times 3{,}10 = 2 \times 5{,}14 = 2 \times 7{,}30 = 2 \times 3 \times 5 \ldots$ of $P(d)$. These oscillations are the reason why the Poisson distribution was not attributed to the NNSD of primes in the past, e.g., $P(2) = P(4) = 1$, while $P(6) = 2$

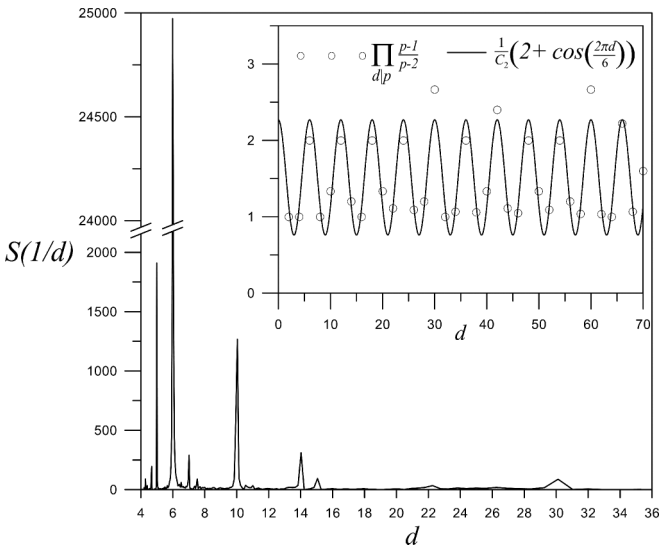

FIG. 2. The plot of power spectrum $S(f)$ calculated from $M = 2^{10} = 1024$ values of $P(d)$ plotted versus $1/f$ to show main periods of $P(d)$. The y axis was broken to make visible peaks at $d \neq 6$. In the inset the plots of $P(d)$ and the approximation (14) are presented.

and the plot should be made with logarithmic scale on the y axis to suppress these oscillations.

In Ref. [31] E. Bombieri and H. Davenport have proved that

$$\sum_{k=1}^{n} \prod_{p|k,\,p>2} \frac{p-1}{p-2} = \frac{n}{\prod_{p>2}\left(1-\frac{1}{(p-1)^2}\right)} + \mathcal{O}(\ln^2(n)), \quad (11)$$

i.e., in the limit $n \to \infty$ the number $2/C_2$ is the arithmetical average of the product $\prod_{p|k} \frac{p-1}{p-2}$. The main period of oscillations is 6; hence, we can write the following:

$$P(d) = \prod_{p|d,\,p>2} \frac{p-1}{p-2} \approx \alpha + \beta \cos\left(\frac{2\pi d}{6}\right). \quad (12)$$

The numerical value of α is equal to $2/C_2$ to reproduce the average value of $P(d)$ in (11). It can be explained by taking into account that $\cos(2\pi 2k/6) = 1$ while $\cos(2\pi(2k+2)/6) = \cos(2\pi(2k+4)/6) = -\frac{1}{2}$ and, hence, by the equation

$$\lim_{n\to\infty} \frac{1}{n} \sum_{k=1}^{n} \left(\alpha + \beta \cos\left(\frac{2\pi 2k}{6}\right)\right) = \alpha, \quad (13)$$

where the value of parameter β does not contribute to the average of the right-hand side of (12). Thus from (11) we have $\alpha = 2/C_2 \approx 1.514\,780\,128\,1$. Requiring that the combination $\alpha + \beta\cos(2\pi d/6)$ for $d = 6$ takes a value 2 times larger than that for $d = 2$ and $d = 4$, $\alpha + \beta = 2(\alpha - \beta/2)$ gives $\beta = \alpha/2 \approx 0.75739$. Fitting of the parameters α and β can be done also numerically by use of standard general linear least squares; see, e.g., Ref. [32]. We have used the procedure

lfit from Ref. [32] with 2 500 000 numbers of points: For $d = 2,4,6,\ldots,5\,000\,000$. The output of the computer run was as follows: $\alpha = 1.51478 \approx 2/C_2, \beta = 0.75471 \approx 1/C_2$. Hence, we propose the compact formula (see inset in Fig. 2) as follows:

$$P(d) = \prod_{p|d,\, p>2} \frac{p-1}{p-2} \approx \frac{1}{C_2}\left(2 + \cos\left(\frac{2\pi d}{6}\right)\right), \qquad (14)$$

which allows us to substitute for $P(d)$ an expression more amenable for algebraic manipulations. Such an approximation may be relevant for calculations of correlations functions for zeros of the Riemann ζ function, where sums involving product $P(d)$ appear very often [33]. It turns out that $\cos(2\pi d/6)$ takes for even d only two values: $-1/2$ for $d = 6k+2$ and $6k+4$ and 1 for $d = 6k$. Because d and d^2 have the same prime divisors it follows that $P(d^2) = P(d)$. The same relation is also obeyed by the approximation (14) because $(6k+2)^2 = 6k' + 4$ and $(6k+4)^2 = 6k'' + 4$ and the square of the $d = 6k$ is obviously again a number of the same form.

The smallest gap between adjacent primes is 2 (twin primes), while the maximal gap $G(x) = \max_{p_n<x}(p_n - p_{n-1})$ grows with x. We can obtain the formula for $G(x)$ from (4) assuming that the largest gap up to x between two consecutive "levels" $p_{n+1} - p_n$ appears only once: $\tau_{G(x)}(x) = 1$. Skipping the oscillating term $P(d)$, which is very often close to 1, we get for $G(x)$ the following estimation expressed directly by $\pi(x)$:

$$G(x) \sim \frac{x}{\pi(x)}(2\ln(\pi(x)) - \ln(x) + c), \qquad (15)$$

where $c = \ln(C_2) = 0.277\,876\,9\ldots$. Substituting here the PNT in the form $\pi(x) \sim x/\ln(x)$ gives the Cramer's conjecture [34] $G(x) \sim \ln^2(x)$ in the limit of large x. The maximal gaps $G(x)$ are scattered chaotically; the largest currently known gap of 1476 follows the prime 1 425 172 824 437 699 411; see Ref. [30]. The comparison of the above formula with real data is presented in Fig. 3.

We finish this section recalling the result of P. Gallagher [35]. He proved, assuming the special generalization of the n-tuple conjecture of Hardy-Littlewood (3), that the fraction of intervals which contain exactly k primes follows a Poisson distribution. More precisely he proved that the number $P_k(h,N)$ of such $n < N$ that the interval $(n, n+h]$ contains exactly k primes is asymptotically for $N \to \infty$ given by

$$P_k(h,N) \sim N\frac{\lambda^k e^{-\lambda}}{k!},$$

where $\lambda \sim h/\ln(N)$ is a parameter of the Poisson distribution. In Ref. [36] E. Kowalski has generalized the Gallagher theorem to other families of primes. In particular, the numbers of twins, primes of the form m^2+1, or Sophie Germain primes (i.e., primes p with $2p+1$ also prime) in short intervals are asymptotically Poisson distributed.

III. UNFOLDED PRIMES

For energy spectrum $E_1, E_2, \ldots$ one usually performs unfolding to focus on fluctuations around the smooth part of staircase and simultaneously to pass to the dimensionless

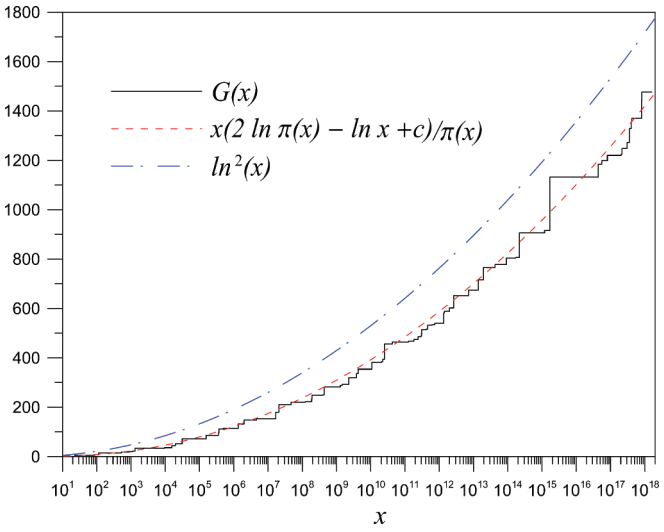

FIG. 3. (Color online) The comparison of $G(x)$ (black solid line) obtained from the computer search (up to $x = 2^{48}$ we have used our own data, and for larger x we took data from the Web pages [30]). For the plot of (15) [red (dark gray) dashed line] we have used the tabulated values of $\pi(x)$ available at Ref. [30]. The plot of the Cramer conjecture is also presented [blue (light gray) dash-dotted line].

variables $e_1, e_2, \ldots$ via the following definition:

$$e_n = \overline{N}(E_n). \qquad (16)$$

Then the average spacing between two consecutive e_n, e_{n+1} is equal to 1 and this procedure removes the individual properties of a system. Although primes are dimensionless we can perform the unfolding using the definition

$$r_n = \mathrm{Li}(p_n). \qquad (17)$$

Then the unfolded spacings are $D_n = r_{n+1} - r_n$, and writing $p_{n+1} = p_n + d_n$ (d_n are "pure" spacings, not unfolded) and using $\mathrm{Li}(x) \sim x/\ln(x)$ we obtain

$$D_n \approx \frac{d_n}{\ln(p_n) + d_n/p_n} \qquad (18)$$

and for large p_n it goes into $D_n = d_n/\ln(p_n)$. In other words, we can say that the unfolded gaps (level spacings) between very large consecutive primes are $D_n = (p_{n+1} - p_n)/\ln(p_n)$. Because the average distance between primes (p_{n-1}, p_n) is $\ln(p_n)$ we have from (18) for large p_n that the average spacing between two consecutive (r_n, r_{n+1}) is equal to 1, as it should be for unfolded variables. The values of D_n are arbitrary real numbers, while d_n assume only even values. For example, for twin primes $p_{n+1} = p_n + 2$ the gap $d = 2$ will be mapped into $D_n \approx 2/\ln(p_n)$ with explicit dependence on p_n and it goes to zero with increasing p_n (if there are infinity of twins, as it is widely believed). On the other side, the maximal value of D will correspond to maximal gaps: From (15) we have that roughly $G(p_n) = \ln^2(p_n)$ and thus the interval of values of D will span up to approximately $\ln(p_n)$: the values $d = 2, 4, 6 \ldots$, $G(x)$ will be mapped onto the interval $[2/\ln(x), \ln(x)]$. To make the histogram of unfolded spacings D_n the (arbitrary) size of bin should be chosen. In this approach the oscillations seen in Fig. 1 are "smeared out" between different bins and there is no possibility to extract them easily from

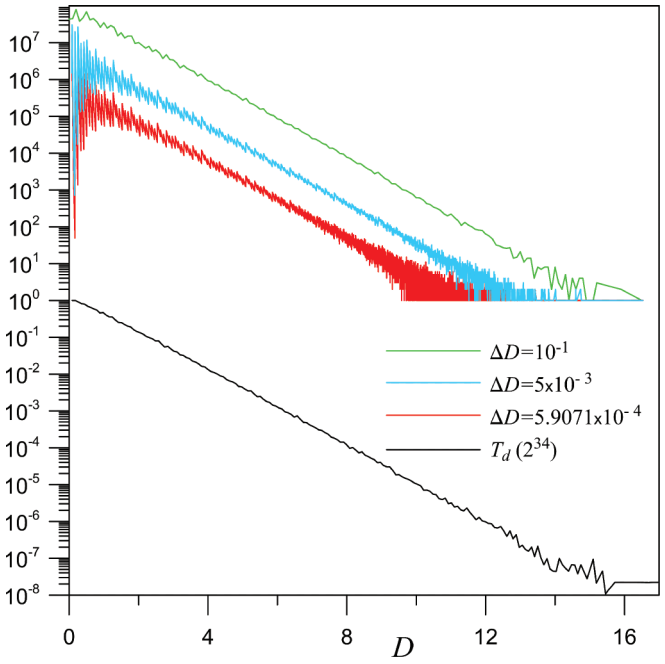

FIG. 4. (Color online) The plot of histograms of unfolded spacings $D_n = r_{n+1} - r_n$ where $r_n = \mathrm{Li}(p_n)$ for primes up to $2^{34} = 1.72\ldots \times 10^{10}$. Three widths of bins are used: $\Delta D = 0.1$ [green (light gray)], $\Delta D = 0.001$ [blue (medium gray)], and $\Delta D = 16.54/28\,000$ [red (dark gray)]. In black (below the legend) is shown the plot for the unfolding defined by Eq. (19).

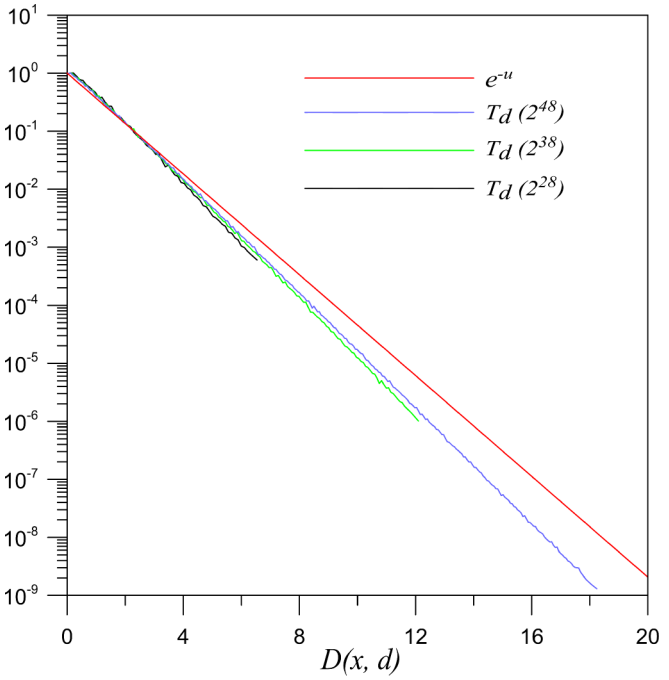

FIG. 5. (Color online) Plots of $(\mathcal{D}(x,d),\mathcal{T}_d(x)),(d = 2,4,\ldots)$ for $x = 2^{28}$ (the bottom, shortest, plot), 2^{38},2^{48} and in red (the longest) the plot of e^{-u} (the order of plots corresponds to the order of descriptions in the legend). Only the points with $\tau_d(x) > 1000$ were plotted to avoid fluctuations at large $D(x,d)$ due to small values of $\tau_d(x)$ for large d.

the histogram of unfolded gaps D_n. The behavior caused by the product $P(d)$ is obscured after the change of variables $d_n \to D_n$; note the oscillations with large amplitude on the red and blue plots in Fig. 4, whereby D_n depends explicitly on the value of p_n and is a continuous variable. In other words, the same bin will contain contributions from different d_n and different p_n, giving the same value of D_n and there is no possibility to untangle for unfolded quantities the influence of the oscillations caused by the product (9). We present the results of this procedure for all primes up to $2^{34} = 1.718\ldots \times 10^{10}$ in Fig. 4 for three choices of the bin size. The popular choice, used, e.g., in EXCEL, is to set the number of bins equal to the square root of the number of values of binned variable. In our case, $\pi(2^{34}) = 762\,939\,111$, thus the number of bins should be approximately 28 000. Because the maximal gap up to 2^{34} is $G(2^{34}) = 382$ and it appears at $p_{486\,570\,087} = 10\,726\,904\,659$, we get that the maximal value of D is $382/\ln(10\,726\,904\,659) = 16.54\ldots$ and the size of bin should be $16.54/28\,000 \approx 0.000\,59$. In Fig. 4 the red (dark gray) line presents the plot for this choice of the bin size, the blue (light gray) line is for the roughly 10 times larger division $\Delta D = 0.005$, while the green (medium gray) plot presents the histogram of prime pairs with D divided into bins of the size $\Delta D = 10^{-1}$. These plots can be normalized by dividing all values by the maximal value present in the histogram for a given bin size.

The explicit form of Eq. (4) allows us to define the unfolding in the following way. Let us define the rescaled quantities as follows:

$$\mathcal{T}_d(x) = \frac{x\tau_d(x)}{C_2 P(d)\pi^2(x)}, \quad \mathcal{D}(x,d) = \frac{d\pi(x)}{x}. \qquad (19)$$

The product $P(d)$ in the denominator of the first formula removes the oscillations and gives the analog of the histogram free of size bin ambiguity. The second equation defines the proper unfolding for prime numbers. Because $x/\pi(x) \approx \ln(x)$ is the mean distance between two consecutive primes $\overline{d} \approx \ln(x)$ up to x, we see that $\mathcal{D}(x,d)$ corresponds to the distances between "unfolded" primes. Normalized spacing between two consecutive primes is $\mathcal{D}(x,d) \approx d/\ln(x)$ and, hence, the mean value of $\mathcal{D}(x,d)$ is simply 1. For large x the quantity $\mathcal{D}(x,d)$ agrees with expression (18) for large p_n: $\mathcal{D}(p_n,d_n) \approx d_n/\ln(p_n) = D_n$ and, hence, values of $\mathcal{D}(x,d) \in [2/\ln(x),\ \ln(x)]$. From conjecture (4) we expect that for each x the points $(\mathcal{D}(x,d),\mathcal{T}_d(x))$, $d = 2,4,\ldots,G(x)$ should coincide—the function $\tau_d(x)$ displays scaling in the physical terminology. In Fig. 5 we have plotted the points $(\mathcal{D}(x,d),\mathcal{T}_d(x))$ for $x = 2^{28},2^{38},2^{48}$ and, indeed, we affirm the tendency of all these curves to collapse into the universal one. To make this plot we have used *exact* values of $\pi(x)$, not any of the approximate formulas like $\mathrm{Li}(x)$. From the definition of $\tau_d(x)$ it follows that $\pi(x) = \sum_d \tau_d(x) + 1$ and it allowes us to calculate from $\tau_d(x)$ precise values of $\pi(x)$ for $x = 2^{28},2^{38},2^{48}$. If we denote $u = \mathcal{D}(x,d)$, then all these scaled functions should exhibit the pure exponential decrease e^{-u}: the Poisson distribution shown in red (dark gray) in Fig. 5. We have determined by use of the least-squares method slope $s(x)$ and prefactor $a(x)$ of the fits $a(x)e^{-s(x)u}$ to the linear parts of plots of $(\mathcal{D}(x,d), \ln(\mathcal{T}_d(x)))$. The results are presented in Fig. 6. The slope very slowly tends to 1: For over 6 orders of x $s(x)$ changes from 1.187 to 1.136 while the prefactor $a(x)$ drops from $1.512\ldots$ to $1.273\ldots$.

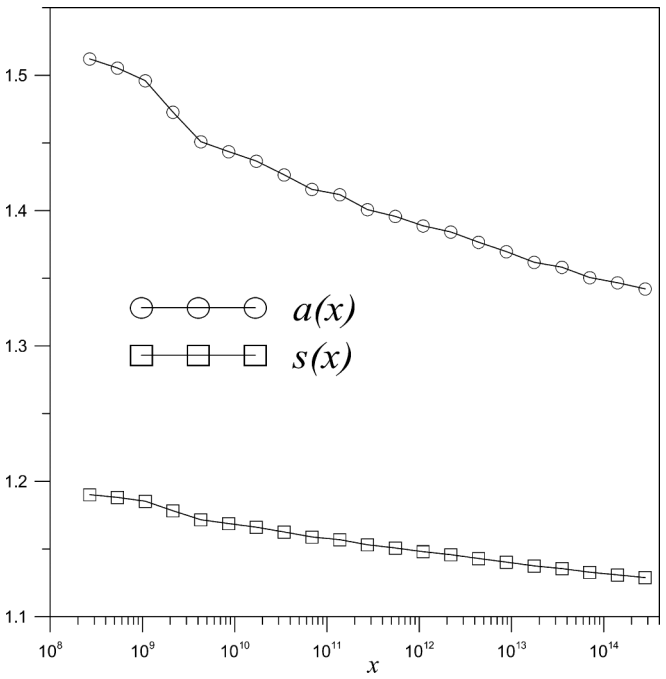

FIG. 6. Plot of slopes $s(x)$ and prefactors $a(x)$ in the dependence $a(x)e^{-s(x)}$ obtained from fitting it to $(\mathcal{D}(d,x), \ln(\mathcal{T}_d(x)))$ for $x = 2^{28}, 2^{29}, \ldots, 2^{48}$.

Finally, let us remark that there is no repulsion of small gaps between primes: usually for GOE or GUE there is a prohibition of small gaps between energy levels (in fact, the number of gaps with $s = 0$ is equal to zero), but for our case the smallest gap corresponds to twins and it is believed that there is infinity of them. From (4) it follows that the number of twins and cousins is roughly half of the number of primes separated by $d = 6$. In fact, for all plots of $\tau_d(x)$ in Fig. 1 $d = 6$ is the highest point, i.e., it is the most often occurring gap. However, in Fig. 1, local spikes appear at multiplicities of $30 = 2 \times 3 \times 5$ and at $d = 210 = 2 \times 3 \times 5 \times 7$, where the product $P(d)$ has local maxima. As x increases, the slopes of plots of $\tau_d(x)$ decrease and at some value around $x \approx 10^{36}$ the peak at $d = 30$ will be greater than that at $d = 6$. At much larger $x \approx 10^{428}$ the spike at 210 will take over $d = 30$. It leads to the so-called problem of champions, i.e., the most occurring gap between consecutive primes; see Ref. [37]. Thus primes are repelled in a very special way: The most often occurring gaps are products of consecutive primes, but they become the "champions" at extremely large values of x. For the unfolded according to Eq. (18) gaps D_n [or Eq. (19) and quantities $\mathcal{D}$ as well] there is no repelling: The most common value of D_n is $2\pi(x)/x \approx 2/\ln(x)$ and it tends to zero with increasing x—behavior typical for the Poisson distribution.

A similar unfolding procedure has been used in dynamical systems, e.g., in the stadium billiard were the existence of strong oscillations due to bouncing ball orbits strongly influence the spectral statistics Δ_3 and, to get a good agreement with the Gaussian orthogonal ensemble (GOE) predictions, one has to perform unfolding, which includes explicitly the contribution of the bouncing ball periodic orbits (see Ref. [38]).

It is a common belief that the Poisson NNSD of the quantum energy levels is linked with integrable systems with more than one degree of freedom. In Ref. [39] P. Crehan has shown that for any sequence of energy levels obeying a certain growth law ($|E_n| < e^{an+b}$, for some $a \in \mathbb{R}^+$, $b \in \mathbb{R}$), there are infinitely many *classically integrable* Hamiltonians for which the corresponding quantum spectrum coincides with this sequence. Because from PNT it follows that the n-th prime p_n grows like $p_n \sim n\ln(n)$, the results of Crehan's paper can be applied and there exist classically integrable Hamiltonians whose spectrum coincides with prime numbers; see also Ref. [11].

IV. SPECTRAL RIGIDITY OF PRIME NUMBERS

In Ref. [40] several statistical measures to describe fluctuations in the energy levels $\{E_n\}$ of complex systems were introduced. One which attracted much attention is the spectral rigidity Δ_3. The spectral rigidity for arbitrary system with spectral staircase $N(E)$ is defined as the averaged mean-square deviation of the best local fit straight line $a\epsilon + b$ to the $N(E)$ on the interval $(x, x + L)$,

$$\Delta_3(x;L) = \frac{1}{L}\left\langle \min_{a,b} \int_0^L (N(x+\epsilon) - a\epsilon - b)^2 d\epsilon \right\rangle. \quad (20)$$

The averaging procedure $\langle\cdot\rangle$ depends on the specific problem, e.g., for random matrices it is the mean value from an ensemble of generated matrices or average over a set of atomic nuclei in real experiments (see, e.g., Ref. [41]); sometimes the average over the initial point x is applied. There are, in general, two ways of performing the operation $\min_{a,b}$; see the discussion in Ref. [40]. One can calculate partial derivatives of right-hand side of (20) with respect to a and b, equate them to zero, solve for a and b, and substitute solutions back to the right-hand side, which leads to the double integrals; see, e.g., Ref. [42] (Appendix II). We will present here the procedure for calculating Δ_3 in this way, which was devised by O. Bohigas and M.-J. Giannoni in Refs. [43] and [20]. First, the energies are unfolded $E_N \to e_n$ using the smooth part $\overline{N}(E_n)$ of the staircase function; see Eq. (16). If the sequence of unfolded levels $e_1, e_2, \ldots, e_n$ falls in the interval $(x, x + L)$, then the following explicit formula for $\Delta_3(x;L)$ is obtained:

$$\Delta_3(x;L) = \frac{n^2}{16} - \frac{1}{L}\left(\sum_{k=1}^{n} \tilde{e_k}\right)^2 + \frac{3n}{2L^2}\sum_{k=1}^{n} \tilde{e_k}^2 - \frac{3}{L^4}\left(\sum_{k=1}^{n} \tilde{e_k}^2\right)^2 + \frac{1}{L}\sum_{k=1}^{n}(n-2k+1)\tilde{e_k}, \quad (21)$$

where $\tilde{e_k} = e_k - (x + L/2)$. In the second approach the parameters a and b are obtained by fitting the straight line $ax + b$ to the set of points $(x_1, y_1), (x_2, y_2), \ldots, (x_n, y_n)$ by use of the least-squares method, i.e., the partial derivatives of $\sum_{k=1}^{n}(y_k - ax_k - b)^2$ with respect to a and b are calculated and put equal to zero, which gives the following very

well-known expressions:

$$a = \frac{n\sum_{k=1}^{n} x_k y_k - \sum_{k=1}^{n} x_k \sum_{k=1}^{n} y_k}{n\sum_{k=1}^{n} x_k^2 - \left(\sum_{k=1}^{n} x_k\right)^2}$$

$$b = \frac{1}{n}\sum_{k=1}^{n}(y_k - a x_k).$$

In the case of $\Delta_3(x;L)$ we have $x_k = E_k, y_k = N(E_k)$. In the spectral rigidity obtained in this second way we will distinguish from (21) by use of an apostrophe, $\Delta_3'(x;L)$. The formula for $\Delta_3'(x;L)$ in this approach and adjusted for our problem will be given below; see (27).

We define spectral rigidity for primes by (20) with $\pi(x)$ instead of $N(x)$. To use the formula (21) the exact values of all primes are needed and we have used primes p_n sufficient for calculation of $\Delta_3(x;L)$ for $x = 10^8, 10^9$, and 10^{10}. To perform the unfolding $p_n \to r_n$ one can use in principle any analytical formula giving the number $\pi(x)$ of primes smaller than x, e.g., the one due to Gauss $\pi(x) \sim x/\ln(x)$ or another one given by the prime number theorem (5): $r_n = \mathrm{Li}(p_n)$. The choice $x/\ln(x)$ is not a good one because $\pi(x) - x/\ln(x)$ never changes the sign (see, e.g., Ref. [44] [Eq. (3.5)]) so there are no oscillations of this difference. Although J. E. Littlewood proved in 1914 [45] that $\pi(x) - \mathrm{Li}(x)$ infinitely often changes the sign, the lowest present-day known estimate for the first sign change of $\pi(x) - \mathrm{Li}(x)$ is around 10^{316} (see Refs. [46] and [47]), hence, in the available for computers range there are no fluctuation of $\pi(x) - \mathrm{Li}(x)$ around zero but a steady growth of the function $\mathrm{Li}(x) - \pi(x)$. In the famous paper [48] B. Riemann has given the *exact* formula for $\pi(x)$ as follows:

$$\pi(x) = \sum_{k=1}^{\infty} \frac{\mu(k)}{k}\left(\mathrm{Li}(x^{\frac{1}{k}}) - \sum_{\rho}\mathrm{Li}(x^{\frac{\rho}{k}}) + \int_{x^{1/k}}^{\infty} \frac{1}{u(u^2-1)\ln(u)}\,du\right), \tag{22}$$

where $\mu(n)$ is the Möbius function as follows:

$$\mu(n) = \begin{cases} 1 & \text{for} \quad n = 1 \\ 0 & \text{when} \quad p^2 | n \\ (-1)^r & \text{when} \quad n = p_1 p_2 \ldots p_r. \end{cases}$$

The sum over ρ runs over nontrivial zeros of the Riemann $\zeta(s)$ function $\zeta(\rho) = 0$ and the last integral contains contribution from trivial zeros $-2m$ of ζ: $\zeta(-2m) = 0, m = 1,2,3,\ldots$. If the Riemann hypothesis is true, then for all nontrivial zeros $\mathrm{Re}(\rho) = \frac{1}{2}$ and the contribution to the sum over k in (22) is dominated by the first term, which leads to the following approximation to $\pi(x)$:

$$R(x) = \sum_{k=1}^{\infty} \frac{\mu(k)}{k}\mathrm{Li}(x^{\frac{1}{k}}). \tag{23}$$

The difference $\pi(x) - R(x)$ changes the sign already at x as low as $x \in [2,100]$ (see, e.g., the tables obtained by T. R. Nicely in Ref. [30]) and up to 10^{14} there are over 50 million sign changes of $\pi(x) - R(x)$ [49]; however, on average, the behavior of both differences $\pi(x) - \mathrm{Li}(x)$ and $\pi(x) - R(x)$ seems to be the same [50]. The above function $R(x)$ can be obtained without the need to calculate the logarithmical integral $\mathrm{Li}(x)$ from the series obtained by J. P. Gram [see, e.g., Ref. [51] (p. 51)]:

$$R(x) = 1 + \sum_{m=1}^{\infty} \frac{\ln^m(x)}{m\,m!\,\zeta(m+1)}. \tag{24}$$

Hence, we have made the unfolding of primes according to the rule

$$r_n = R(p_n). \tag{25}$$

At this point let us remark that from (6) and (24) we see that, because $\zeta(m) \to 1$ for $m \to \infty$, very quickly [e.g., $\zeta(4) = \pi^4/90 = 1.082\,323\ldots, \zeta(6) = \pi^6/945 = 1.017\,343\ldots$] for large x the functions $\mathrm{Li}(x)$ and $R(x)$ should differ by roughly $\ln\ln(x)$, and this quantity can be discarded in comparison with values of series involving powers of $\ln(x)$ present in (6) and (24). Indeed, from (23) it follows using the first term from asymptotic expansion (5) that for large x the approximate relation $R(x)/\mathrm{Li}(x) = 1 - 1/\sqrt{x}$ holds. Thus for large x the particular form of unfolding (17) or (25) should be irrelevant, despite the fact that $\pi(x) - \mathrm{Li}(x)$ changes the sign for the first time somewhere in the vicinity of $x = 10^{316}$ while $\pi(x) - R(x)$ changes the sign already for x between 10 and 20 (see the tables in Nicely [30]).

We will present the plots of $\Delta_3(x;L)$ for three values of x: $10^8, 10^9$, and 10^{10}. The values of primes for which the unfolded variables begin to fall into the intervals $(10^8, 10^8 + L)$, $(10^9, 10^9 + L)$, and $(10^{10}, 10^{10} + L)$ are, accordingly, 2 038 076 627, 22 801 797 631, and 252 097 715 777: $R(2\,038\,076\,627) = 10^8 + 1.8496\ldots, R(22\,801\,797\,631) = 10^9 + 2.3178\ldots, R(252\,097\,715\,777) = 10^{10} + 0.0024\ldots$. As there seems to be no clear relation between the values of L in comparison with chosen x we have used the wide range of values of L: We have calculated from (21) spectral rigidity for values $L = 2^7 = 128, \ldots, 2^{26} = 67\,108\,864$. The results are presented in Fig. 7. It is well known that for the stationary Poisson ensemble $\Delta_3(x;L) = \frac{L}{15}$ (see, e.g., Ref. [40] [Eq. (61)] or Ref. [42] (Appendix II)) and in the Fig. 7 this theoretical prediction is plotted in red (straight line). The obtained plots of $\Delta_3(x;L)$ seem to tend to the line $L/15$ with increasing x. For primes there is no natural averaging procedure present in the definition (20) and in Fig. 7 prominent fluctuations are seen. To simulate the averaging we have performed the following "Monte Carlo" experiment for $x = 10^{10}$. From the PNT in the form $\pi(k) \sim k/\ln(k)$ it follows that the chance that the randomly chosen large integer k should be a prime is $1/\ln(k)$. Such a probabilistic model for primes was created by H. Cramer in the 1930s [34]. We have started to test if a given natural k number is the probabilistic "artificial" prime from the first k_0 for which $R(k_0) > 10^{10}$, i.e., for $k_0 = 252\,097\,715\,777$, for which $R(k_0) = 10^{10} + 0.002\,41\ldots$. The natural number $k > k_0$ [even the even numbers were allowed—when even numbers are skipped the probability of odd number k to be a "prime" should be $2/\ln(k)$] was accepted to be a "probabilistic" prime if $1/\ln(k)$ was larger than that uniformly generated from the interval $(0,1)$ random number random: random $< 1/\ln(k)$. For such a "prime" k the unfolding was performed using the equation $r_k' = R(k)$. The random drawing of "primes" was continued until the unfolded "prime" was larger than $x + L$

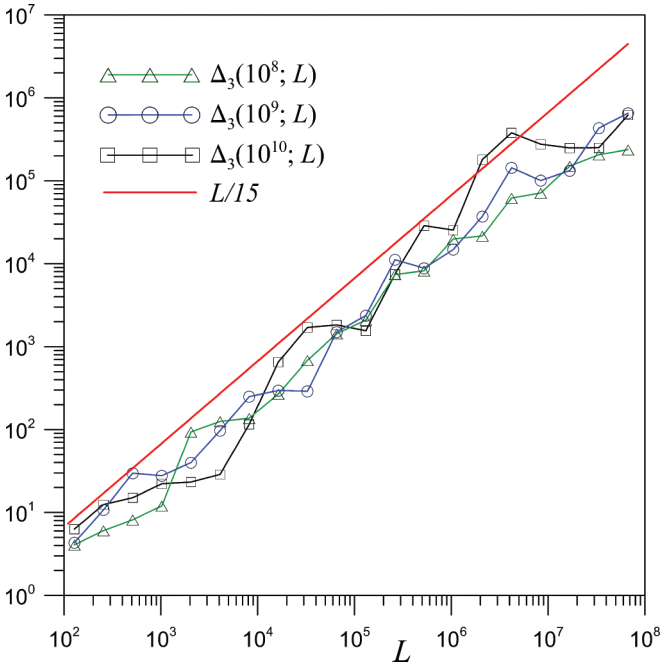

FIG. 7. (Color online) Plots of $\Delta_3(x; L)$ obtained from (21) for $x = 10^8$ (triangles), $x = 10^9$ (circles), and $x = 10^{10}$ (squares) and $L = 2^7 = 128, \ldots, 2^{26} = 67\,108\,864$.

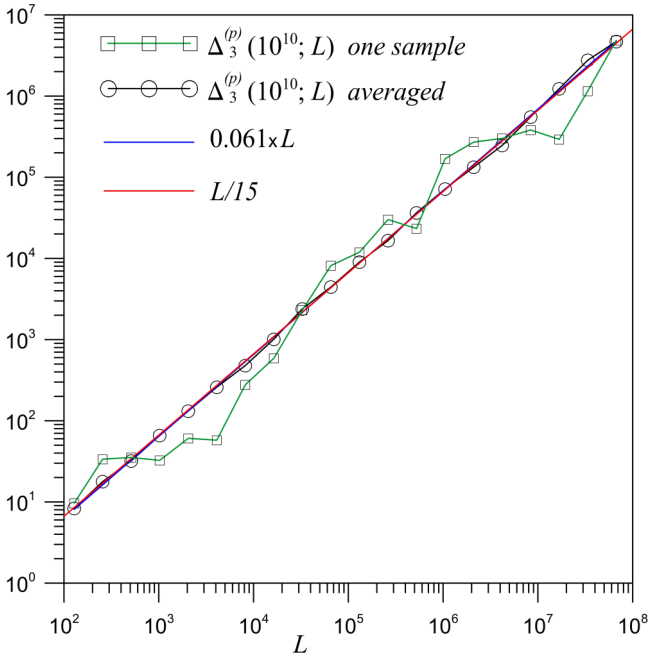

FIG. 8. (Color online) The plot of $\Delta_3^{(p)}(L)$ for probabilistic primes for one particular realization of the "artificial primes" in green (boxes) and averaged over 100 samples in black (circles). The last plot perfectly coincides with the red (dark gray) line representing $L/15$. In blue (light gray) is the fit $0.061L$ to circles plotted (practically indistinguishable from straight line $L/15 = 0.066\ldots \times L$).

for $L = 128, \ldots, 2^{26}$. For the set of such generated unfolded quantities in the intervals $(x, x + L)$ the "artificial" spectral rigidity $\Delta_3^{(p)}(x; L)$ was calculated using (21). The result of this procedure is plotted in green (squares) in Fig. 8 and there are fluctuations seen resembling those present in Fig. 7 for "true" primes. But now we can generate many independent sets of the artificial probabilistic primes. We have repeated this procedure 100 times and the averaged over all these samples spectral rigidity $\Delta_3^{(p)}(x; L)$ is presented in Fig. 8 in black (circles). Now the fluctuations have disappeared and the obtained plot follows perfectly the predicted dependence $L/15$. This allows us to claim that the spectral rigidity for prime numbers unfolded via the Riemann function $R(x)$ is the same as that for Poisson statistics [we have checked that the same result is obtained for unfolding with $\mathrm{Li}(x)$ as in Eq. (17)]. Let us mention that usually saturation of Δ_3 is observed in physical systems, i.e., after the initial dependence resembling $L/15$ spectral rigidity stops to increase and is constant for large L (see, e.g., Ref. [23] or Ref. [52]). However, our system is infinite and there is no departure from the straight line $L/15$.

Next we will present spectral rigidity for the second method of minimizing the right-hand side of (20) over a, b, namely determination of a, b by use of the least-squares method. In the case of prime numbers, for large x, the smooth part of staircase $\pi(x)$ given by $x/\ln(x)$ is almost linear in the interval $(x, x + L)$ as the denominator changes from $\ln(x)$ to $\ln(x + L) = \ln(x) + L/x + \cdots$, which for $x \gg L \gg 1$ again is $\ln(x)$. There are a few Web sites [30] offering the tables of values of $\pi(x)$ (as well as other number-theoretic functions). In these data files the values of $\pi(x)$ are tabulated with different step sizes of x; the best resolution is at A. V. Kulsha's page: the file pi.txt (421 MB) contains counts of $\pi(x)$ with a step of 10^9 from $x = 10^9$ to $x = 2.5 \times 10^{16}$. Now we will give the formula for calculating the integral appearing in the definition of $\Delta_3'(x; L)$ as follows:

$$\mathcal{I}(x; L) = \int_0^L (\pi(x + \epsilon) - a\epsilon - b)^2 d\epsilon, \tag{26}$$

which is appropriate for our data. Let us assume that the values of $\pi(x)$ in the integral (26) are known with the resolution h: $y_k = \pi(x + kh)$. Hence, we assume that $\pi(x)$ is constant on the intervals $(kh, (k + 1)h)$ [in fact, $\pi(x)$ is constant only between two consecutive primes]. We regard this sampling of $\pi(x)$ with different steps h as the averaging procedure hidden in the angle bracket in (20)—taking values of $\pi(x)$ at all consecutive primes would introduce fluctuations. The combination $\pi(x + \epsilon) - a\epsilon - b$ is the linear function on the intervals $(kh, (k + 1)h)$ and we can write (we assume here that L is the integer multiple of h) the following:

$$\begin{aligned}\mathcal{I}(x; L) &= \int_0^L (\pi(x + \epsilon) - a\epsilon - b)^2 d\epsilon \\ &= \sum_{k=0}^{L/h-1} \int_{kh}^{(k+1)h} (y_k - a\epsilon - b)^2 d\epsilon.\end{aligned}$$

Performing elementary integration we obtain the following:

$$\Delta_3'(x; L) = b^2 + abL + \frac{a^2L^2}{3} + \frac{1}{L}\sum_{k=0}^{L/h-1} y_k(y_k - 2b)h - ay_k(2k + 1)h^2. \tag{27}$$

It should be noted that parameters a and b in Eq. (27) obtained from fitting $a\epsilon + b$ to points $\pi(x+\epsilon), 0 \leqslant \epsilon \leqslant L$ by use of the least-squares method are functions of L and x; see below (29).

The value of $\Delta_3'(x;L)$ given by (27) should not depend on h. To test this presumption we have calculated $\Delta_3'(x;L)$ for $x_1 = 10^{13}$ and $x_2 = 10^{16}$ and for $h_1 = 10^9$, $h_2 = 2\times10^9$, and $h_3 = 4\times10^9$. We have chosen the following sequence of values of the length of intervals $L = 16h_1 = 1.6\times10^{10}$, $32h_1 = 3.2\times10^{10}, \ldots 2^{23}h_1 = 8.388\,608\times10^{15}$ for both x_1,x_2 and, additionally, $L = 1.5\times10^{16}$ for $x_2 = 10^{16}$. It means that the number of terms in the sum in (27) was, appropriately, $2^3, 2^4, \ldots, 2^{22} = 4194304$ for h_2 and $2^2, 2^4, \ldots, 2^{21} = 209\,715\,2$ for h_3. For each L the parameters a and b were fitted by use of the least-squares method to the points $[x_k = x + kh, y_k = \pi(x+kh)], k = 0,1,\ldots,L/h-1$. In Figs. 9 and 10 we present the results. Two types of behaviors are seen in these figures: the constant in L values of Δ_3' depending on h and the collapse of plots of Δ_3' for all h when the increase of Δ_3' with L begins. It seems that to get rid of dependence on h the sufficiently large number L/h of terms in the formula (27) has to be summed up. Inspection of the data shows that, to have the independence of Δ_3' on h, a few thousand terms in the sum in (27) are sufficient (for the largest L there are millions of terms in this sum; see the plots in red in Figs. 9 and 10). It is possible to find heuristically the values of the constant in L parts of Δ_3'. To find the analytical expressions for a and b we consider the smooth part of $\pi(x)$ given by $(x+\epsilon)/\ln(x+\epsilon)$ and the straight line $a\epsilon + b$ obtained by best fitting to the values of $(x+kh)/\ln(x+kh)$.

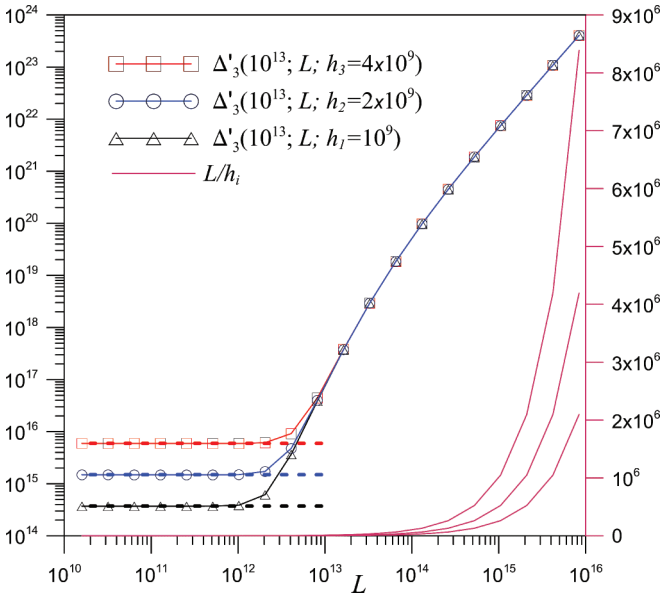

FIG. 9. (Color online) Plots of $\Delta_3'(x_1;L;h)$ for $x_1 = 10^{13}$ and $L = 16h_1 = 1.6\times10^{10}, 32h_1 = 3.2\times10^{10}, \ldots 2^{23}h_1 = 8.388\,608\times10^{15}$ and three values of $h_1 = 10^9$ (black triangles), $h_2 = 2h_1$ (blue circles) and $h_3 = 4h_1$ (red squares). On the right in purple (no symbol) are plotted values of the number of terms $L/h_i - 1$ in the sum (27) and the right y axis also in purple (no symbol) is for these numbers. The dashed lines represent values of (31). The coincidence of $\Delta_3'(x_1;L)$'s for all h_i starts at approximately $L = 2^{14}h_1 = 1.6384\times10^{13}$.

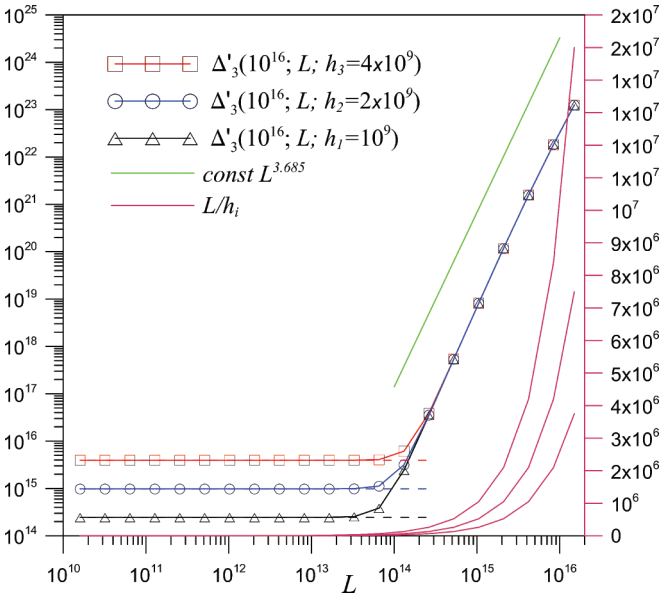

FIG. 10. (Color online) Plots of $\Delta_3'(x_2;L;h)$ for $x_1 = 10^{16}$ and $L = 16h_1 = 1.6\times10^{10}, 32h_1 = 3.2\times10^{10}, \ldots 2^{23}h_1 = 8.388\,608\times10^{15}$ and additionally for $L = 1.5\times10^{16}$ and three values of $h_1 = 10^9$ (black triangles), $h_2 = 2h_1$ (blue circles), and $h_3 = 4h_1$ (red squares). On the right in purple (medium gray) are the plotted values of the number of terms $L/h_i - 1$ in the sum (27) and the right y axis, also in purple, is for these numbers. The dashed lines represent values of (31). The coincidence of $\Delta_3'(x_2;L)$'s for all h_i starts at approximately $L = 2^{18}h_1 = 2.621\,44\times10^{14}$ and follows practically powerlike increase given by equation $2.569\,5\times10^{-37}L^{3.685}$. The green (light gray) line presents this equation multiplied by 100; however, we expect bending of $\Delta_3'(x_2;L;h)$ for $L > x_2$ similar to the one seen in Fig. 9.

The experiments show that the fits cross $(x+\epsilon)/\ln(x+\epsilon)$ on the interval $\epsilon \in (0,L)$ roughly at $\epsilon = L/4$ and $\epsilon = 3L/4$ (see Fig. 11), thus from $(x+L/4)/\ln(x+L/4) = aL/4 + b$ and $(x+3L/4)/\ln(x+3L/4) = a3L/4 + b$ we get

$$a = \frac{2}{L}\left[\frac{x+3L/4}{\ln(x+3L/4)} - \frac{x+L/4}{\ln(x+L/4)}\right] = \frac{1}{\ln(x)} - \frac{L}{2x\ln^2(x)} + O(1/x^2), \tag{28}$$

$$b = \frac{x+L/4}{\ln(x+L/4)} - aL/4 = \frac{x}{\ln(x)} - \frac{L}{4\ln^2(x)} + O(1/x). \tag{29}$$

Using $y_k = (x+kh)/\ln(x+kh) \approx (x+kh)/\ln(x) - (kh)^2/2x\ln^2(x)$ we obtain in (27) sums over k which can be calculated exactly, and retaining the leading terms gives the following:

$$\Delta_3'(x;L) = \frac{h^2}{3\ln^2(x)} - \frac{hL}{4\ln^3(x)} + O(1/x). \tag{30}$$

Because $\Delta_3'(x;L) > 0$ we have from above $h^2/3\ln^2(x) > hL/4\ln^3(x)$, i.e., $L < 4h\ln(x)/3$, which for $x = 10^{13}$ gives $L < 40h$. Surprisingly, the first term in (30), not depending on

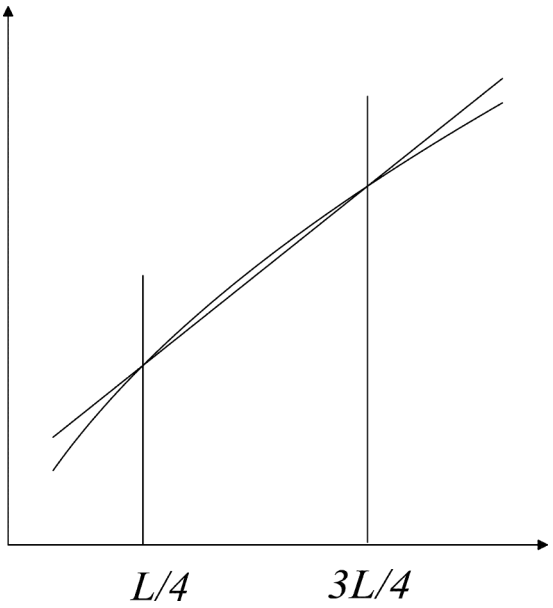

FIG. 11. The illustration of the experimental fact that the straight line best fitting $(x+\epsilon)/\ln(x+\epsilon)$ on the interval $\epsilon \in (0, L)$ crosses it at $\epsilon = L/4$ and $\epsilon = 3L/4$.

L but being the function of x, gives the expression

$$\Delta_3'(x; L; h) = \frac{h^2}{3\ln^2(x)} + \cdots, \tag{31}$$

which works very well, even for $L = 1024h$ for $x_1 = 10^{13}$ and $L = 8192h$ for $x_2 = 10^{16}$, as shown in Figs. 9 and 10, where the predicted values $h^2/3\ln^2(x)$ are plotted by dashed lines together with the plots of $\Delta_3'(x; L; h)$ obtained from (27). In fact, this agreement is astonishing: e.g., all $\Delta_3'(10^{16}; L; h_1)$ for the initial 11 values of L have the same first three digits: $2.455\ldots \times 10^{14}$, while (31) predicts $2.455\,88\ldots \times 10^{14}$. In Fig. 9 we were able to make the plot for L up to almost $10^3 x_1$, while in Fig. 10 the largest L is smaller than x_2; thus we expect bending of $\Delta_3'(x_2; L; h)$ for larger L, similar to the behavior of $\Delta_3'(x_1; L; h)$ in Fig. 9. In the plots of Δ_3' we see the crossover at value L^*, above which the steeper increase of spectral rigidities begins and this dependence is L^γ, with $\gamma \approx 3.1$. Heuristically, the existence of this crossover can be justified by the following reasoning: For moderate values of L the straight line $a\epsilon + b$ approximates $\pi(x+\epsilon)$ quite well, leading to the small values of the integral $\int_x^{x+L}[\pi(x+\epsilon) - a\epsilon - b]^2 d\epsilon$, while for larger L the discrepancy between $\pi(x+\epsilon)$ and the straight line increases, leading to larger values of Δ_3. The spectral rigidity calculated in the second way displays behavior that differs from $\Delta_3(x; L)$ obtained in the first manner. Let us remark at this point that the proof of $\Delta_3(x; L) = L/15$ for the Poisson ensemble was obtained in Ref. [42] (Appendix 42) only for the first method of minimalization over a and b in (20).

V. CONCLUSIONS

In this paper we have treated prime numbers as energy levels and we applied the physical methods used to study spectra of quantum systems to the description of distribution of prime numbers. We presented large numerical data (up to $x = 2.814\ldots \times 10^{14}$) in support of the formula (4) for the NNSD between consecutive primes. It was also possible to obtain the analytical formula (15) for the maximal difference between two adjacent primes smaller than x. The case of prime numbers gives us the rare opportunity to calculate spectral rigidity $\Delta_3(x; L)$ for the wide range of x and L: For real physical systems usually only hundreds (nuclei), thousands, or hundreds of thousands of (e.g., billiards) energies are known. As the main result of this paper, we regard the scaling relations (19) and attempt to calculate spectral rigidity $\Delta_3(x; L)$ for prime numbers. We have proposed a method to average the spectral rigidity over realizations of probabilistic primes and, after sampling over 100 sets of "artificial" primes, we have obtained perfect $L/15$ dependence. The obtained results confirm that the primes follow the Poisson distribution. This averaging shows that the spectral rigidity does not depend on peculiarities of the primes but on the probability $1/\ln(k)$ of the number k to be prime. The entire above analysis can be repeated for subsets of prime numbers, for example, for the twin primes (both p and $p+2$ are prime), cousin primes (both p and $p+4$ are prime), or the primes of the form $4k^2+1$; in the latter case, the "energy levels" are the values of k for which $4k^2+1$ is prime.

ACKNOWLEDGMENTS

I thank Marek Kuś, Jonathan Sondow, and Karol Życzkowski for comments and remarks. I also thank anonymous referees for useful comments and suggestions.

[1] M. Wolf, Physica A **160**, 24 (1989).
[2] Z. Gamba and J. Hernando, Phys. Lett. A **141**, 106 (1990).
[3] M. Wolf, Physica A **241**, 493 (1997).
[4] B. L. Lan and S. Yong, Physica A **334**, 477 (2004).
[5] P. Billingsley, Am. Math. Mon. **80**, 1099 (1973).
[6] M. Wolf, Physica A **250**, 335 (1998).
[7] C. C. Bonanno and M. Mega, Chaos Solitons Fractals **20**, 107 (2004).
[8] G. Mussardo, arXiv:cond-mat/9712010 (1997).
[9] S. K. Sekatskii, arXiv:0709.0364 (2007).
[10] D. Schumayer, B. P. van Zyl, and D. A. W. Hutchinson, Phys. Rev. E **78**, 056215 (2008).
[11] H. C. Rosu, Mod. Phys. Lett. A **18**, 1205 (2003).
[12] R. L. Liboff and M. Wong, Int. J. Theor. Phys. **37**, 3109 (1998).
[13] T. Timberlake, Am. J. Phys. **74**, 547 (2006).
[14] T. Timberlake and J. Tucker, arXiv:0708.2567 (2007).
[15] W. Arendt and W. P. Schleich, *Mathematical Analysis of Evolution, Information and Complexity* (Wiley-VCH, Weinheim, 2009).
[16] F. Haake, *Quantum Signatures of Chaos*, 2nd ed., Springer Series in Synergetics (Springer-Verlag, Berlin, 2001).
[17] M. L. Mehta, *Random Matrices*, 2nd ed. (Academic Press, San Diego, CA, 1991).

[18] H. A. Weidenmüller and G. E. Mitchell, Rev. Mod. Phys. **81**, 539 (2009).
[19] M. V. Berry and M. Robnik, Am. J. Phys. A **17**, 2413 (1984).
[20] O. Bohigas and M.-J. Giannoni, in *Mathematical and Computational Methods in Nuclear Physics*, edited by J. Dehesa, J. Gomez, and A. Polls, Vol. 209 of Lecture Notes in Physics (Springer, Berlin, 1984), pp. 1–99.
[21] B. Cipra, What is Happening in the Mathematical Sciences (AMS) **4**, 2 (1999).
[22] A. Terras, *Zeta Functions of Graphs* (Cambridge University Press, Cambridge, UK, 2011).
[23] M. V. Berry, Proc. R. Soc. A **400**, 229 (1985).
[24] G. H. Hardy and J. E. Littlewood, Acta Math. **44**, 1 (1922).
[25] M. McKee, Nature (2013), doi:10.1038/nature.2013.12989.
[26] J. Maynard, arXiv:1311.4600 (2013).
[27] M. Wolf, Physica A **274**, 149 (1999).
[28] M. Abramowitz and I. A. Stegun, *Handbook of Mathematical Functions with Formulas, Graphs, and Mathematical Tables* (Dover, New York, 1964).
[29] D. A. Goldston and A. H. Ledoan, Integers **12B**, 1 (2012/13).
[30] Web pages with tabulated values of $\pi(x)$, http://www.trnicely.net, http://www.ieeta.pt/~tos/primes.html, http://sage.math.washington.edu/home/kstueve/A_V_KULSHA.
[31] E. Bombieri and H. Davenport, Proc. R. Soc. A **293**, 1 (1966).
[32] W. H. Press, B. P. Flannery, S. A. Teukolsky, and W. T. Vetterling, *Numerical Recipes: The Art of Scientific Computing* (Cambridge University Press, New York, 1986).
[33] E. Bogomolny and J. Keating, Nonlinearity **8**, 1115 (1993).
[34] H. Cramer, Acta Arith. **II**, 23 (1937).
[35] P. Gallagher, Mathematika **23**, 4 (1976).
[36] E. Kowaslki, Acta Arith. **148**, 153 (2011).
[37] A. Odlyzko, M. Rubinstein, and M. Wolf, Exp. Math. **8**, 107 (1999).
[38] M. Sieber, U. Smilansky, S. C. Creagh, and R. G. Littlejohn, Am. J. Phys. A: Math. Gen. **26**, 6217 (1993).
[39] P. Crehan, J. Phys. A: Math. Gen. **28**, 6389 (1995).
[40] M. L. Mehta and F. J. Dyson, J. Math. Phys. **4**, 701 (1963).
[41] R. U. Haq, A. Pandey, and O. Bohigas, Phys. Rev. Lett. **48**, 1086 (1982).
[42] A. Pandey, Ann. Phys. **119**, 170 (1979).
[43] O. Bohigas and M.-J. Giannoni, Ann. Phys. **89**, 393 (1975).
[44] J. B. Rosser and L. Schoenfeld, Illinois J. Math. **6**, 64 (1962).
[45] J. Littlewood, Comptes Rendus **158**, 1869 (1914).
[46] C. Bays and R. Hudson, Math. Comput. **69**, 1285 (2000).
[47] Y. Saouter and P. Demichel, Math. Comput. **79**, 2395 (2010).
[48] B. Riemann, in *Monatsberichte der Berliner Akademie* (Ferd. Dummler's Verlag–Buchhandlung, Berlin, 1859), pp. 671–680 [English translation available at: http://www.maths.tcd.ie/pub/HistMath/People/Riemann].
[49] T. Kotnik (private communication).
[50] T. Kotnik, Adv. Comput. Math. **29**, 55 (2008).
[51] H. Riesel, *Prime Numbers and Computer Methods for Factorization* (Birkhuser, Boston, 1994).
[52] G. Casati, B. V. Chirikov, and I. Guarneri, Phys. Rev. Lett. **54**, 1350 (1985).